

Supplementary Data

4 Ahmed M.R.H. Mostafa^{1,a}, Ahmed G. Hemdan^{1,2,a}, Praneeth R. Kuninty^{1,a}, Tushar N Satav¹, Maike
5 Spijkerman¹, Ran Li^{3,4}, David Lagares⁵, Franck Assayag⁶, Miles Miller^{3,4}, Jai Prakash^{1,7*}

⁷ ¹Engineered Therapeutics, Advanced Organ Bioengineering and Therapeutics, Department of Bioengineering
⁸ Technology, TechMed Centre, University of Twente, Enschede, The Netherlands.

⁹ ²Department of Pharmacology and Toxicology, Faculty of Pharmacy, Assiut University, Egypt.

10 ³Department of Radiology, Massachusetts General Hospital and Harvard Medical School, Boston, MA, USA.

11 ⁴Center for Systems Biology, Massachusetts General Hospital Research Institute, Boston, MA, USA.

12 ⁵Center for Immunology and Inflammatory Diseases, Division of Rheumatology, Allergy and Immunology,
13 Massachusetts General Hospital, Harvard Medical School, Boston, MA, USA.

14 ⁶Central animal handling laboratory, TechMed Centre, University of Twente, 7500AE, Enschede, The
15 Netherlands.

16 ⁷ScarTec Therapeutics BV, 7522LW, Enschede, The Netherlands.

17

18 ^a Shared authorship

19

20 *Corresponding address:

21 Engineered Therapeutics section

22 Department of Bioengineering Technology

23 TechMed Centre

24 University of Twente

25 7500 AE, Enschede

26 The Netherlands

27 T (+31)-53-489 3096

28 Email: J.Prakash@utv.ac.in

Supplementary Data

29 **Supplementary material**

30 **Molecular docking analysis**

31 To predict the binding sites of AV3 peptidomimetic with $\alpha 5\beta 1$, we performed molecular docking using the
32 Autodock vina version 1.2.0 default protocol ⁴⁹. The AV3 peptidomimetic sequence was drawn using Malvern
33 software and docked with (PDB: 7NLW, without ligand). Auto Dock vina analyses docking simulations,
34 including visualizing conformations, conformational similarity, and interactions between ligands and proteins,
35 as well as the affinity potentials created by Auto Grid, placed with the following dimensions: center_x=270.03,
36 center_y=262.47, center_z=256.54. Docking was performed with energy range = 3, exhaustiveness = 8 to obtain
37 the top 5 best poses with the protein. The ligand-protein interaction images were developed using PyMOL
38 software ver. 2.5.5 (Schrodinger, LLC).

39
40

41 **RNA isolation and qPCR**

42 hPSC were seeded in 12 well plate (4×10^4 cells/well) in complete medium. The next day, cells were starved,
43 and a day later, cells were treated with human transforming growth factor beta (TGF- β 1) (5ng/ml) for 24 h.
44 Then, the cells were lysed, and the total RNA was isolated using Nucleospin RNA isolation kit (Bioké,
45 Netherlands). Then, we synthesized cDNA using iScriptTM cDNA Synthesis Kit (BioRad, Netherlands). Finally,
46 PCR reaction was performed using 10 ng for each reaction. The real-time PCR primers (Table 1) for human
47 α SMA (ACTA2), ITGA5 & RPS18 were purchased from Sigma Aldrich (The Netherlands). The fold change
48 induction was normalized to the gene expression level of RPS18 as a house keeping gene.

49
50 **Supplementary Table 1:** List of primers for quantitative real-time PCR

Gene	Forward primer	Reverse primer
α -SMA	CCCCATCTATGAGGGCTATG	CAGTGGCCATCTCATTTC
ITGA5	CAACTTCTCCTTGGACCCCC	GTCCTCTATCCGGCTTTGC
Collal	GTACTGGATTGACCCCAACC	CGCCATACTCGAACTGGAAT
CD44	AGGAACCTGCAGAATGTGGA	GTAAAGTGTCCCAGCTCCCT
ABCC1	TTCCCCTGAACATTCTCCCC	CATTCCCTCACGGTGATGCTG

Supplementary Data

BCL2	GTCTGGGAATCGATCTGGAA	AATGCATAAGGCAACGATCC
KRAS	GAGGCCTGCTGAAAATGACTG	ATTACTACTGCTTCCTGTAGG
MMP-2	AGGAGGAGAAGGCTGTGTC	CTCCAGTTAAGGCGGCATC
MMP-9	TCTTCCCTGGAGACCTGAGA	TTTCGACTCTCCACGCATCT
WNT-1	CCTCCACGAACCTGCTTACA	TCCCCGGATTTGGCGTATC
CXCL-1	ATGCCAGCCACTGTGATAGA	TCCCCTGCCCTCACAAATGAT
CSF-3	TAGCGGCCTTTCCTCTACC	CAGTTCTCCATCTGCTGCC
IL-1 β	CAGAAGTACCTGAGCTCGCC	AGATTCGTAGCTGGATGCCG
RPS18	TGAGGTGGAACGTGTGATCA	CCTCTATGGGCCCGAATCTT

51

52

Supplementary Table 2: List of primary and secondary antibodies

Antibody	Source	Dilution
Mouse monoclonal β -actin	Thermo Fisher Scientific	1:5000
Rat polyclonal CD31	Southern Biotech	1:50
Mouse monoclonal YAP antibody	Santa Cruz	1:50
CXCL-12 polyclonal Antibody	Santa Cruz	1:50
Anti-STUB1/CHIP antibody	Abcam	1:250
IL-6 Polyclonal Antibody	Thermo Fisher Scientific	1:100
mouse monoclonal anti-HIF-1 alpha	R&D Systems	1:100
Anti-collagen type 1	Southern Biotech	1:250
Alexa Flour TM488 donkey anti-mouse	Thermo Fisher Scientific	1:100
Alexa Flour TM549 donkey anti-rabbit	Thermo Fisher Scientific	1:100
Alexa Flour TM488 donkey anti-rabbit	Thermo Fisher Scientific	1:100
Alexa Flour TM488 donkey anti-goat	Thermo Fisher Scientific	1:100
HRP-conjugated goat anti-rabbit IgG	DAKO	1:2000
HRP-conjugated goat anti-mouse IgG	DAKO	1:2000

53

Supplementary Data

54 AV3-Cy3/IR680 conjugation and HPLC characterization

55 AV3-Cy3 conjugation: AV3-PEG-NH₂ (0.1mg) was dissolved in 5 μ l of DMSO and added to 40 μ l of PBS. Cy3-
56 NHS (0.2mg) was dissolved in 10 μ l of anhydrous DMSO and added to the peptidomimetic solution, then pH
57 was adjusted to 7.4. For, AV3-IR680 conjugation, AV3-PEG-NH₂ (0.29mg) was dissolved in 10 μ l of DMSO
58 and added to 75 μ l of 10x PBS (pH adjusted to 7.4). IR680 NHS (0.25mg) was dissolved in 10 μ l of anhydrous
59 DMSO and added dropwise to the peptidomimetic solution and reacted at 4°C for 16 h.
60 The resulting mixture solutions were purified by 2kDa dialysis cassette and confirmed the conjugate construct
61 using HPLC. The HPLC method used an Ultimate® 3000 uHPLC (Thermo Scientific) equipped with a UV/vis
62 detector (λ = 280/555nm) and C18 UPLC column.

63

64 Liposomes preparation

65 Lipids and dyes were purchased commercially as follows: 1,2-dimyristoyl-sn-glycero-3-phosphocholine
66 (DMPC, Sigma Aldrich), Cholesterol (Sigma Aldrich), 1,2-distearoyl-sn-glycero-3-phosphoethanolamine-N-
67 [carboxy(polyethylene glycol)-2000] (DSPE-PEG-COOH, Avanti Polar Lipids, Alabama, USA), 1,2-
68 distearoyl-sn-glycero-3-phosphoethanolamine-N-[polyethylene glycol)-2000] (DSPE-PEG, Sigma Aldrich),
69 1,2-distearoyl-sn-glycero-3-phosphoethanolamine-N-[carboxy(polyethylene glycol)-2000] (DSPE-PEG-NH₂,
70 Sigma Aldrich), IRDye®, CW800 NHS Ester (LI-COR, Lincoln, NE, USA), 1,1'-Dioctadecyl-3,3,3',3'-
71 Tetramethylindocarbocyanine Perchlorate ('DiI'; DiIC18(3), Thermo Fischer Scientific).

72 Liposomes were prepared based on the ethanol injection technique⁴⁹. For *in vitro* uptake studies, lipid solutions
73 of DMPC: Cholesterol: DSPE-PEG: DSPE-PEG-COOH: DiI at a molar ratio of 6.5: 3: 0.45: 0.05: 0.02 were
74 used. For *in vivo* studies, DSPE-PEG-NH₂ lipid was modified with CW800 NHS in the presence of 0.004%
75 triethanolamine, the reaction mixture was reacted at room temperature for 2 h. The lipid solutions of DMPC:
76 Cholesterol: DSPE-PEG: DSPE-PEG-COOH at the molar ratio of 6.5: 3: 0.422: 0.05 were added to the modified
77 DSPE-PEG-CW800 lipid. For all liposomal formulations, the lipid mixtures were dissolved in ethanol at 30°C.
78 Crude liposomes were formed by mixing the warm lipid mixture with PBS (1:10, vol: vol) under constant vortex.
79 The crude liposomal size was reduced by repeated extrusion through a polycarbonate membrane (Whatman,
80 UK), pore size 200nm, 100nm, using an Avastin Lipofast extruder. After preparation, liposomes were purified

Supplementary Data

81 using a PD10 column (GE healthcare). The liposome size (in PBS) and zeta potential (in 10mM KCl) were
82 measured using Zetasizer Nano ZS (Malvern, UK). The liposomes were stored at 4°C
83

84 AV3 peptide conjugation to liposomes

85 Liposomes were purified, and their buffer was exchanged to MES buffer (pH=6.3) using PD-10 columns (GE
86 Healthcare, Little Chalfont, UK). Next, the COOH group on DSPE-PEG-COOH was activated using a 50x
87 molar excess of N-hydroxysulfosuccinimide (Sulfo-NHS, Sigma Aldrich) and 1-ethyl-3-(3-dimethyl
88 aminopropyl)carbodiimide hydrochloride (EDC, Sigma Aldrich) for 45 mins at RT on a roller. Next, the buffer
89 was changed to 10x PBS (pH=7.4), and excess of EDC and NHS was removed using a PD-10 column (GE
90 Healthcare). Afterward, AV3-NH₂ was added to the liposomes using 2,5x molar excess of peptides compared
91 to DSPE-PEG-COOH and reacted overnight at 4°C. To block unreacted sulfo-NHS esters, the liposomes were
92 incubated with 12,5x molar excess of glycine compared to DSPE-PEG-COOH and reacted for 1 h at RT.
93 Subsequently, unreacted peptides and glycine were removed by 3 times washing with 30 kDa Amicon columns
94 (Sigma Aldrich).

95 96 In vitro cellular binding of nanoparticles

97 hPSC were seeded in a density 2 x 10⁴ cells per well in 12 well-plate and activated with 5 ng/ml human
98 recombinant TGF-β1 (myCAF) or 1 ng/ml of IL-1α (iCAF). Cells were PBS-washed and incubated with
99 detaching buffer containing 0.5% BSA and 5 mM of Ethylenediaminetetraacetic acid (EDTA; Sigma-Aldrich)
100 in PBS for 15. Then, cells were washed and incubated with blocking buffer, composed of 0.9% sodium azide,
101 0.5% BSA and 2 mM EDTA in PBS for 30 mins. Later, cells were incubated with DiI-labelled nanoparticles in
102 blocking buffer for 60 mins. Next, cells were washed by the blocking buffer and samples were run on
103 MACSQuant® flow cytometer (Miltenyi Biotec. Bergisch Gladbach, Germany).

104 105 3D heterospheroid model

106 Heterospheroids were generated by co-culturing PANC-1 and PANC-1 + hPSC (1:5), respectively in a balanced
107 1:1 (v/v) mixture of complete DMEM and stellate cell medium. Cells were seeded in a density of 6 x 10³ cells
108 per well in 96-well round bottom plates coated with 1% Pluronic F-127 (Sigma Aldrich). The growth of

Supplementary Data

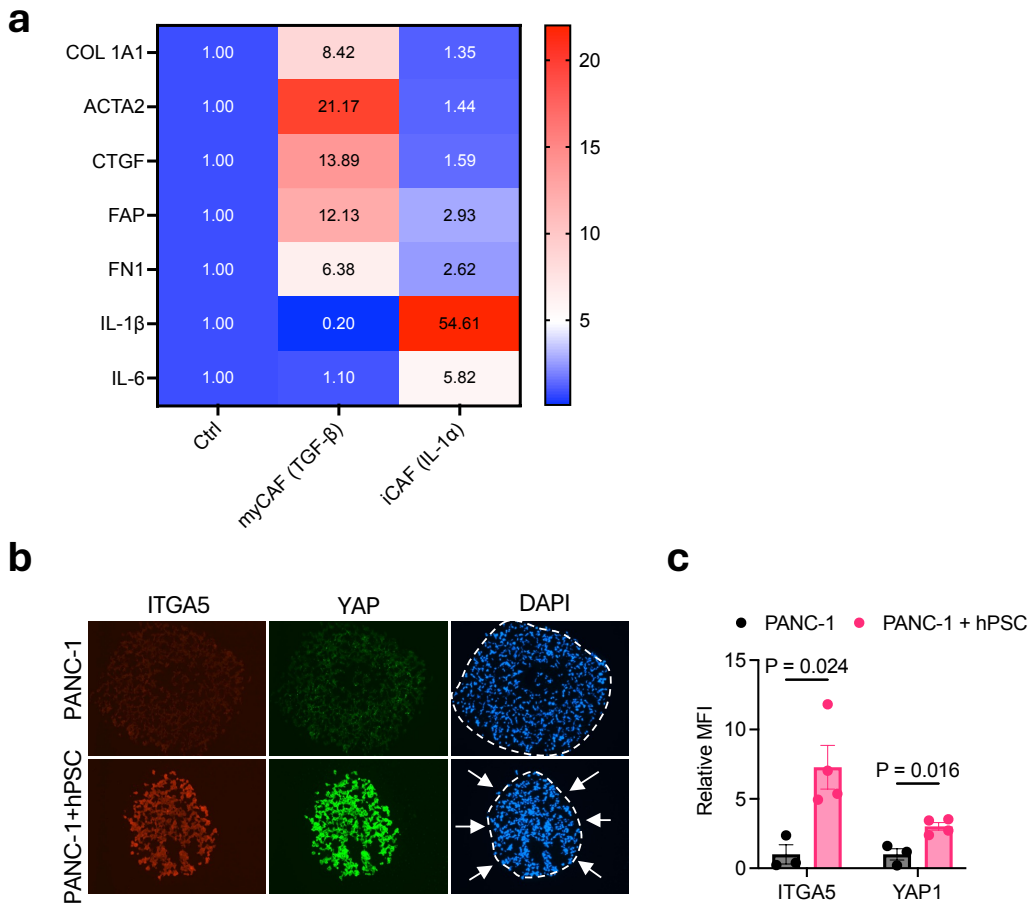
109 spheroids were followed using an inverted microscope after the treatment with YL-109 and/or gemcitabine. To
110 examine the effect on gene expression, spheroids were isolated and processed for the gene expression analyses
111 using qPCR. CTglo assay was performed to determine %ATP.

112
113

Supplementary Data

114 **Supplementary Figures**

115



116

117

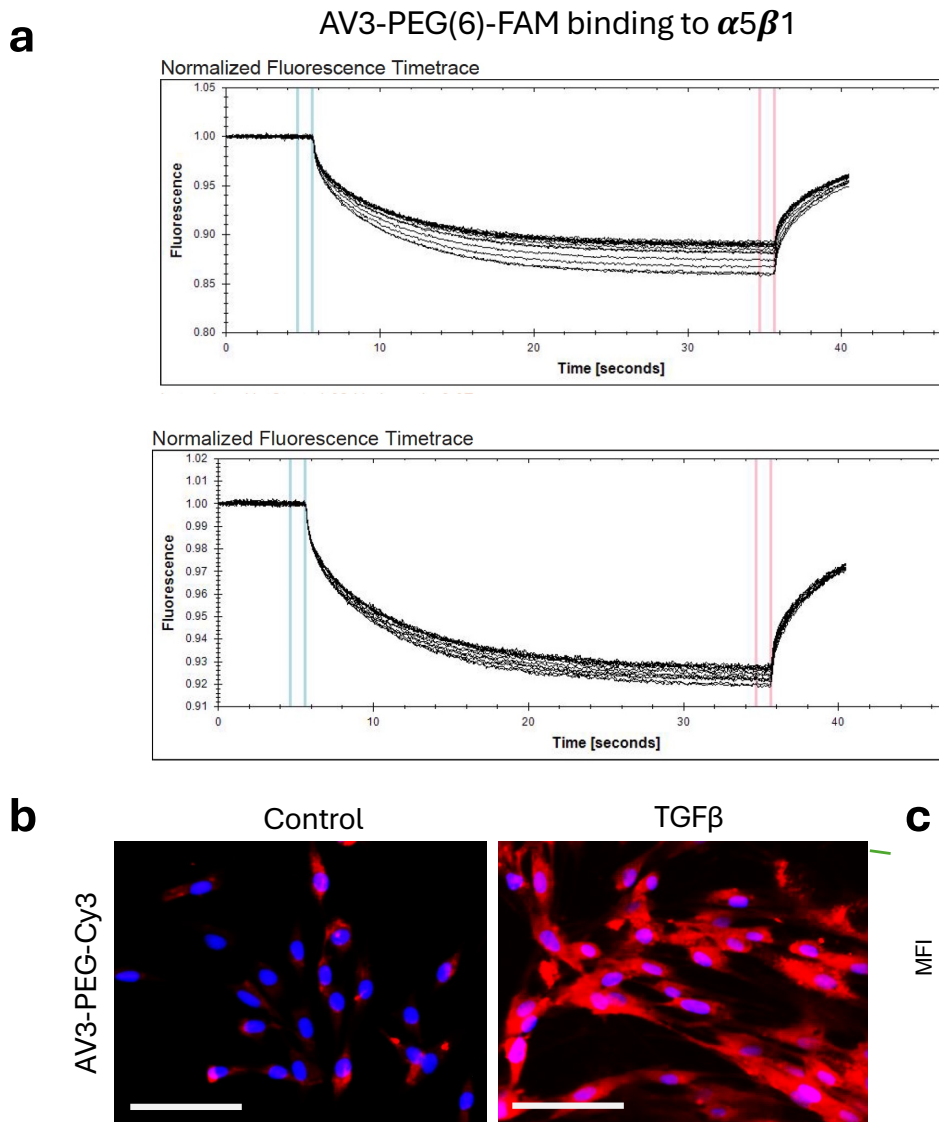
118 **Supplementary Figure 1. (a)** Heatmap showing mRNA expression for different markers related to myCAF
 119 and iCAF upon treatment with TGF- β 1 and IL-1 α in human pancreatic stellate cells. Data represent the mean
 120 for two independent experiments. **(b)** Representative immunofluorescence microscopic images showing the
 121 expression of ITGA5 and YAP in 3D heterospheroids (PANC-1+hPSC) compared to 3D homospheroids
 122 (PANC-1). Quantitative analyses of the staining show a significant increase in the expression. Statistical
 123 analysis was performed using unpaired student's t test for multiple comparison.

124

125

126

Supplementary Data



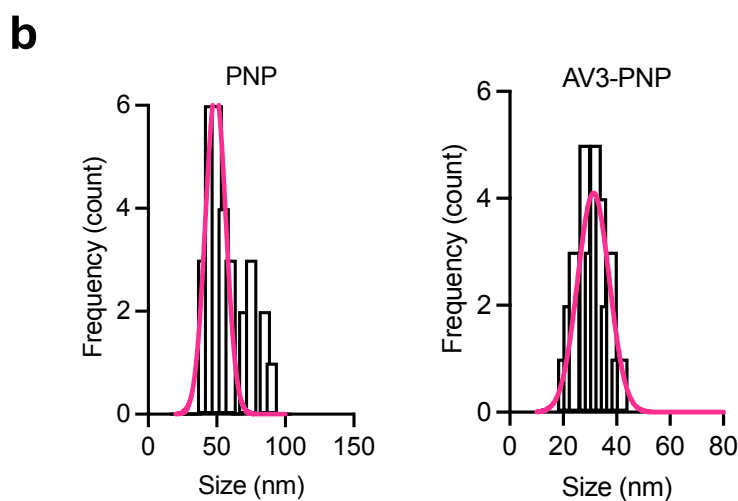
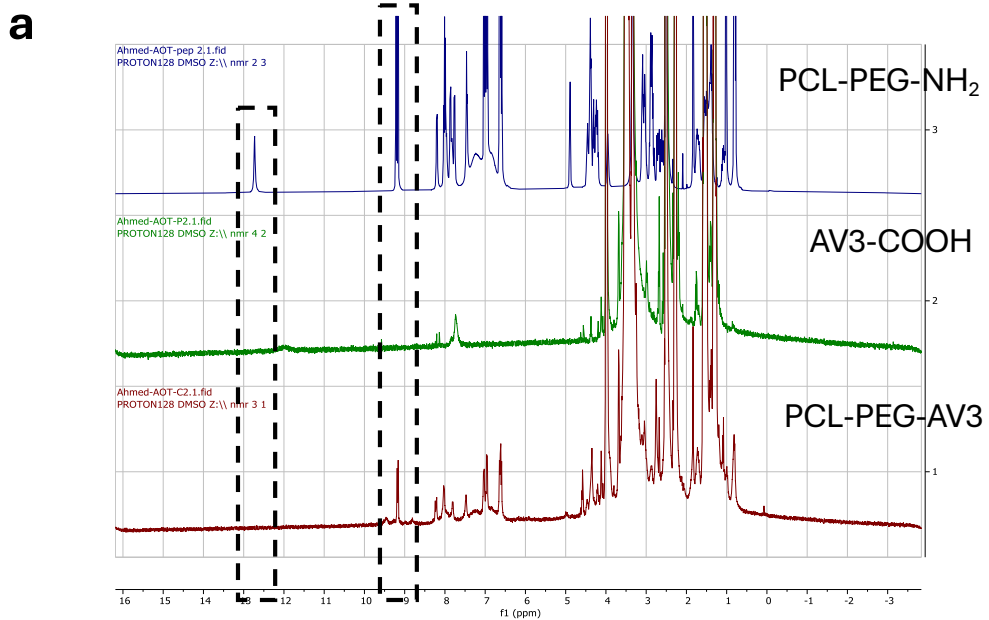
127

128 **Supplementary Figure 2.** (a) Fluorescence time traces for AV3-PEG(6)-FAM binding to human recombinant
 129 $\alpha 5\beta 1$ (upper) and $\alpha 4\beta 1$ (lower) receptors using microscale thermophoresis analysis. (b) Fluorescence
 130 microscopic images showing binding of AV3-PEG(6)-cy3 (10 μ M) to hPSC with/without the activation with
 131 TGF β 1. Scale bar 100 μ m. (c) violin graphs show the quantitation data with flow cytometry at 0.5 μ M
 132 concentration.

133

134

Supplementary Data



135

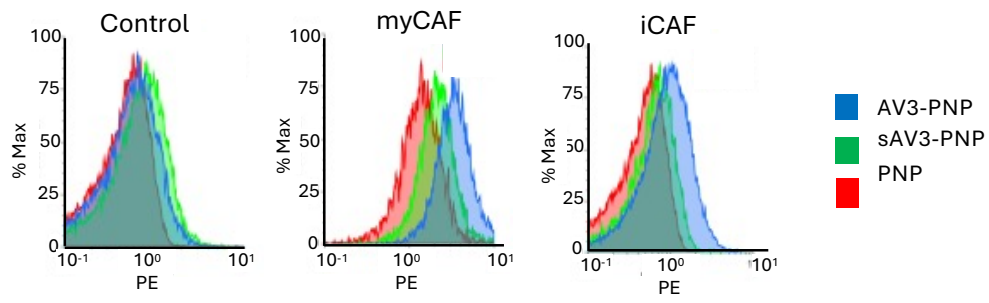
136 **Supplementary Figure 3. Characterization of AV3-functionalized PCL-PEG and AV3 nanoparticles. (A)**

137 Proton NMR spectra of PCL-PEG-NH₂ (blue), AV3 (green) and the PCL-PEG-AV3 conjugate (red). Dotted
138 box indicates free -COOH proton peak.

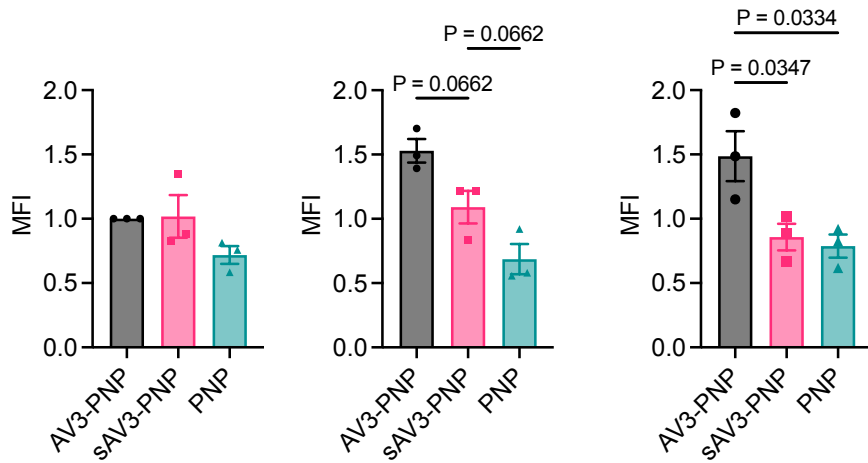
139

140

a



b



141

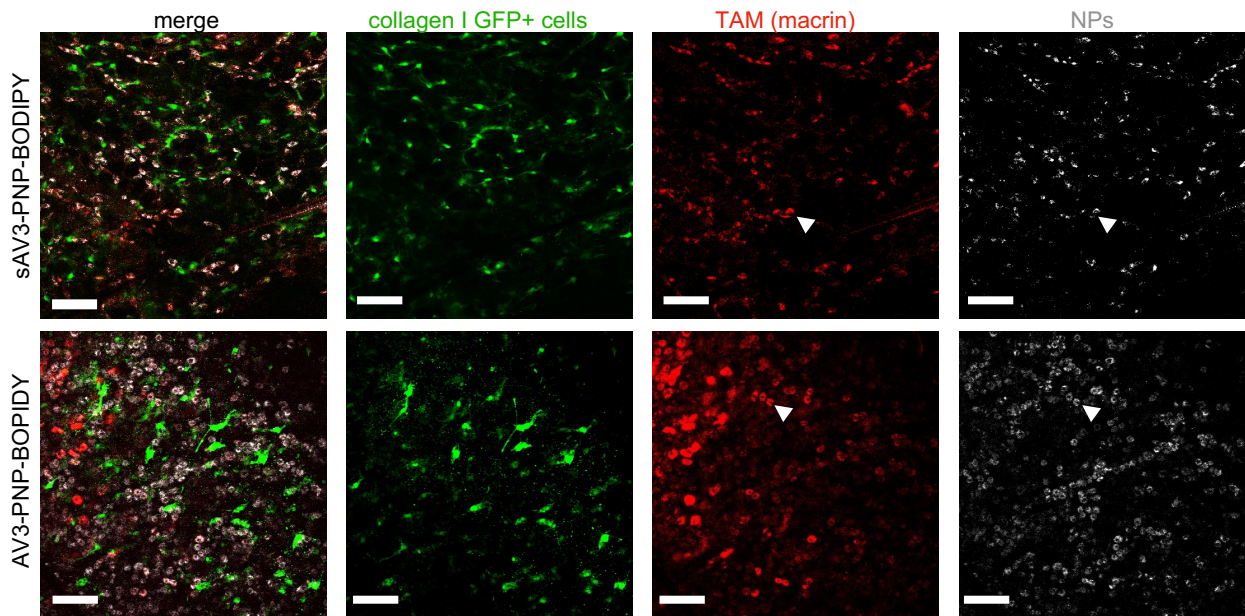
142

143 **Supplementary Figure 4.** (a) Flow cytometry histograms and (b) quantitative analysis for the binding of
 144 fluorescence dye-labelled nanoparticles to quiescent hPSC, myCAF (TGF- β -activated) and iCAF (IL-1 α -
 145 activated). Data represent mean \pm SEM ($n=3$). One-Way ANOVA with multiple comparison corrected by Holm
 146 Sidak test.

147

148

Supplementary Data



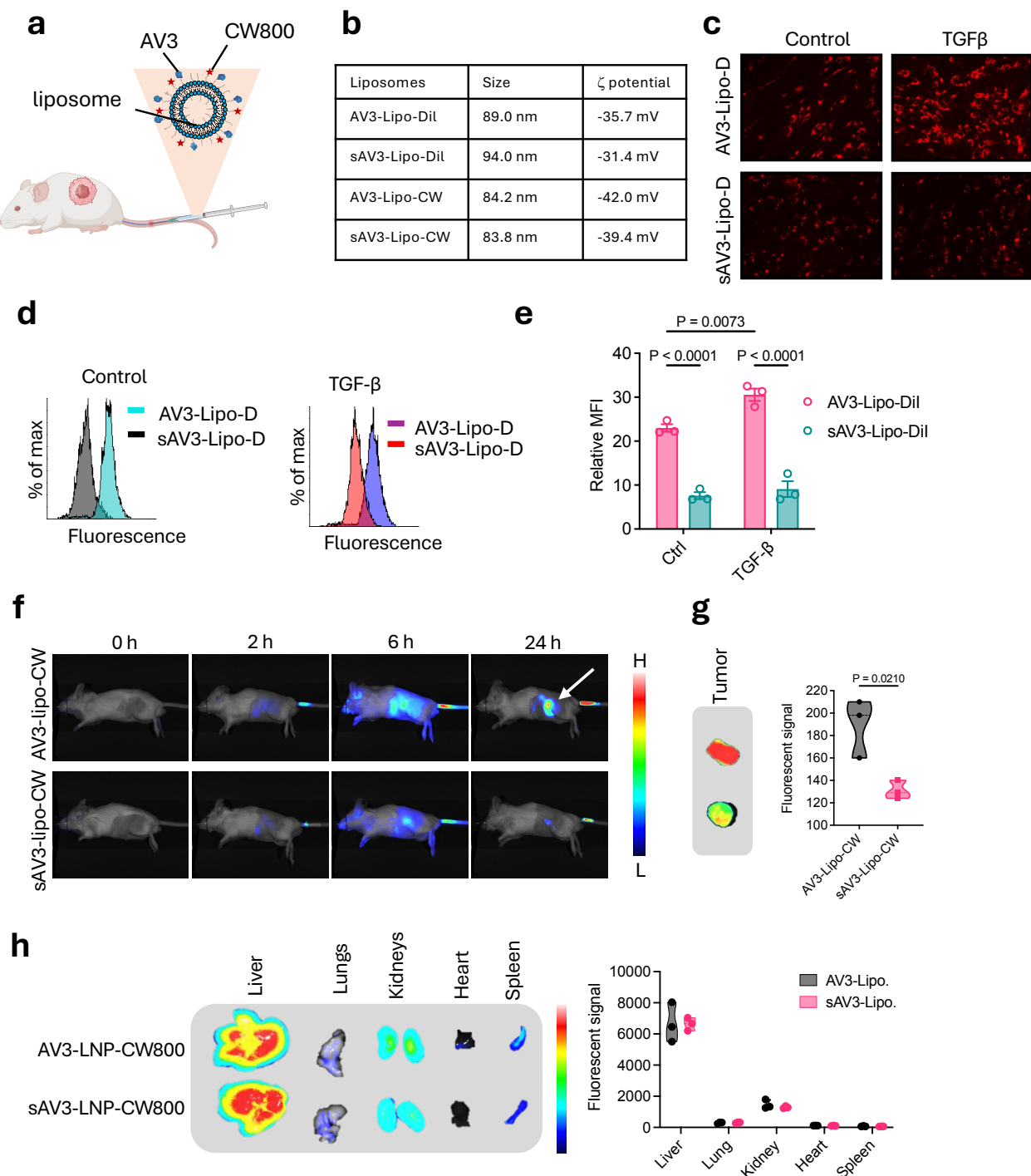
149

150 **Supplementary Figure 5.** Multi-colour fluorescence microscopic images showing the co-localization of AV3-
151 PNP-BODIPY and sAV3-PNP-BODIPY with CAFs (EGFP+ green cells) and TAMs (Macrin+ red cells) in
152 KPC tumour bearing transgenic collagen-1 α 1-EGFP+ mice at t=24 h after the intravenous injection. Scale bar:
153 100 μ m. (b) Scatter graphs and histograms for the flow cytometry analysis showing the gating schemes and
154 differences for the uptake of RhB-labelled different nanoparticles (AV3-PNP, sAV3-PNP, PNP) by myCAF,
155 iCAF and TAMs in vivo.

156

157

Supplementary Data



158

159 **Supplementary Figure 6.** **(a)** Schematic illustration showing AV3-conjugated liposomes modified with
 160 CW800 NIR dye or encapsulating DiI dye. **(b)** Size and zeta potential of typical liposomal formulations. **(c)**
 161 Fluorescence microscopic images and **(d, e)** showing the uptake of AV3-Lipo-Dil and sAV3-Lipo-Dil in hPSC
 162 with/without TGF- β 1 treatment. Mean \pm s.e.m. n=3. Two-Way ANOVA corrected with Holm Sidak method.
 163 **(f)** In vivo NIR imaging of mice injected with AV3 or sAV3 conjugated liposomes labelled with CW800 NIR

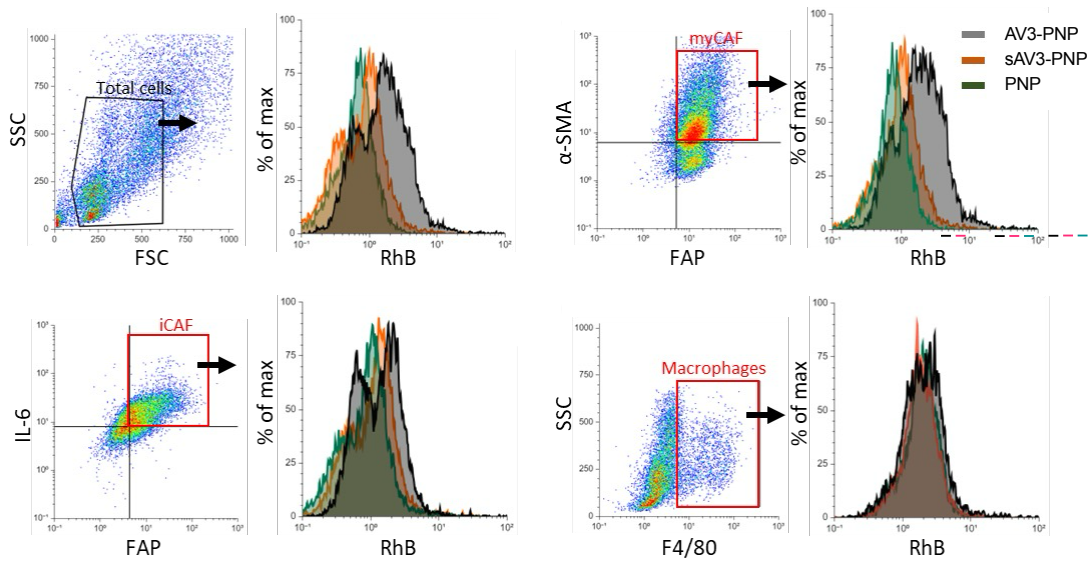
Supplementary Data

164 dye in co-injection PDAC model until t=24h. **(g)** Representative NIR images and quantitation of the isolated
165 tumours. Data present n=3 mice per group. Statistical analysis was performed using two-sided unpaired t test.
166 **(h)** Representative NIR images and quantitation of different organs from n=3 mice per group. Data present n=3
167 mice per group. Statistical analysis was performed using multiple comparison two-sided unpaired t test. No
168 significance was found.

169

170

Supplementary Data



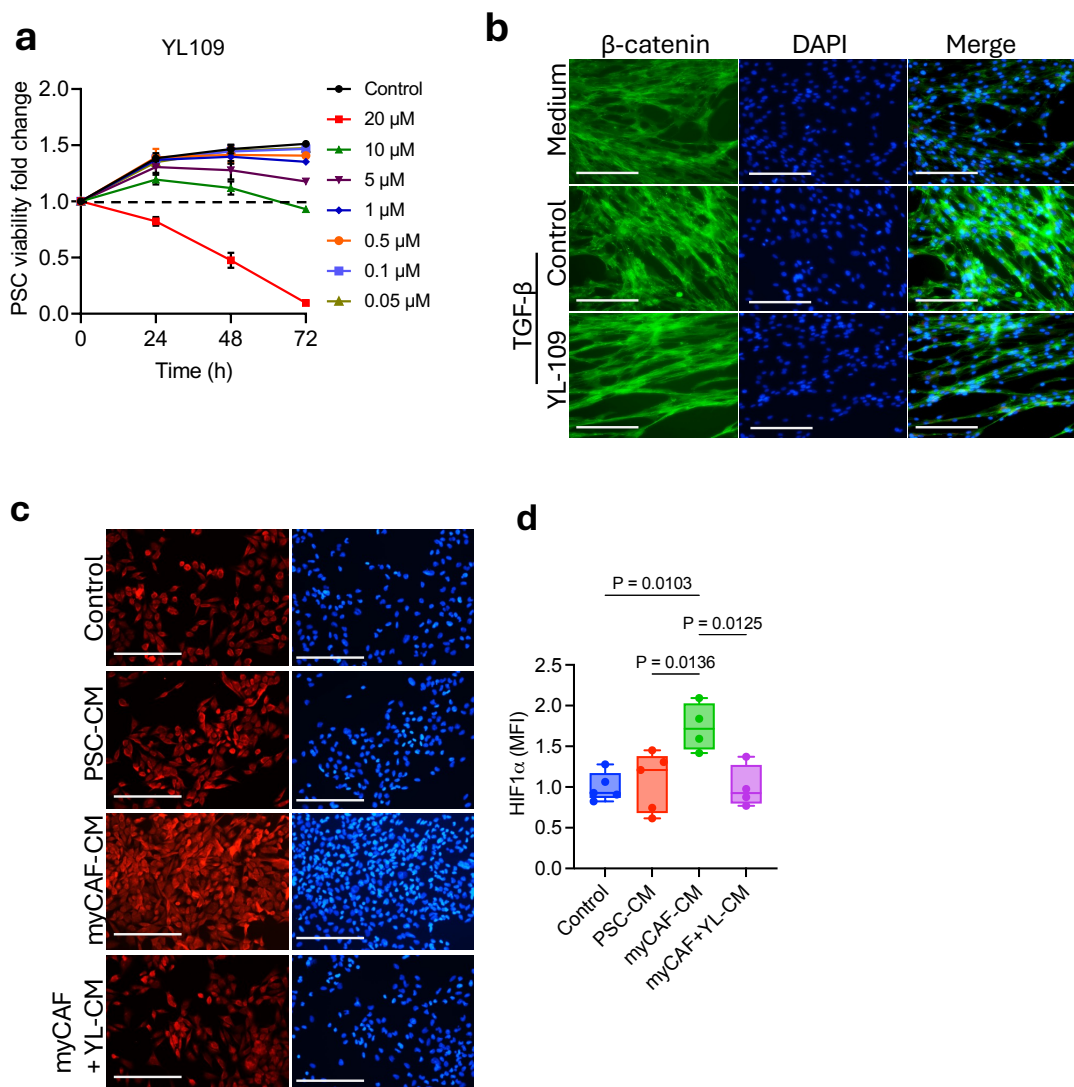
171

172

173 **Supplementary Figure 7.** Scatter graphs and histograms for the flow cytometry analysis showing the gating
174 schemes and differences for the uptake of RhB-labelled different nanoparticles (AV3-PNP, sAV3-PNP, PNP)
175 by myCAF, iCAF and TAMs in vivo.

176

177



178

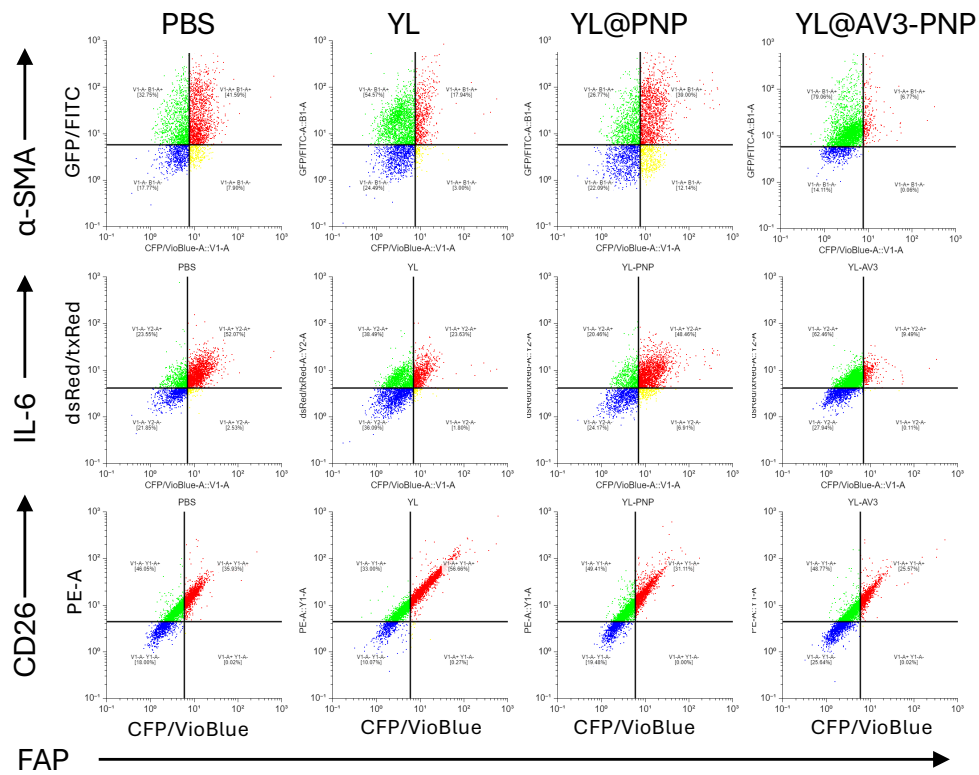
179

180 **Supplementary Figure 8. YL109 inhibits TGF- β -induced overexpression of beta catenin.** (a) 181 Representative fluorescence microscopy images and (b) quantification of β -catenin expression by TGF- β - 182 activated hPSC. Scale bar: 200 μ m. Graphical data represent mean \pm s.e.m. (n=3). (c, d) Immunofluorescence 183 staining and quantitation of HIF-1 α in PANC-1 cells treated with conditioned media collected from either hPSC, 184 myCAFs (TGF- β treated) or myCAF-treated with YL-109. Blue colour represents DAPI staining in nuclei. 185 Scale bar: 100 μ m.

186

187

Supplementary Data



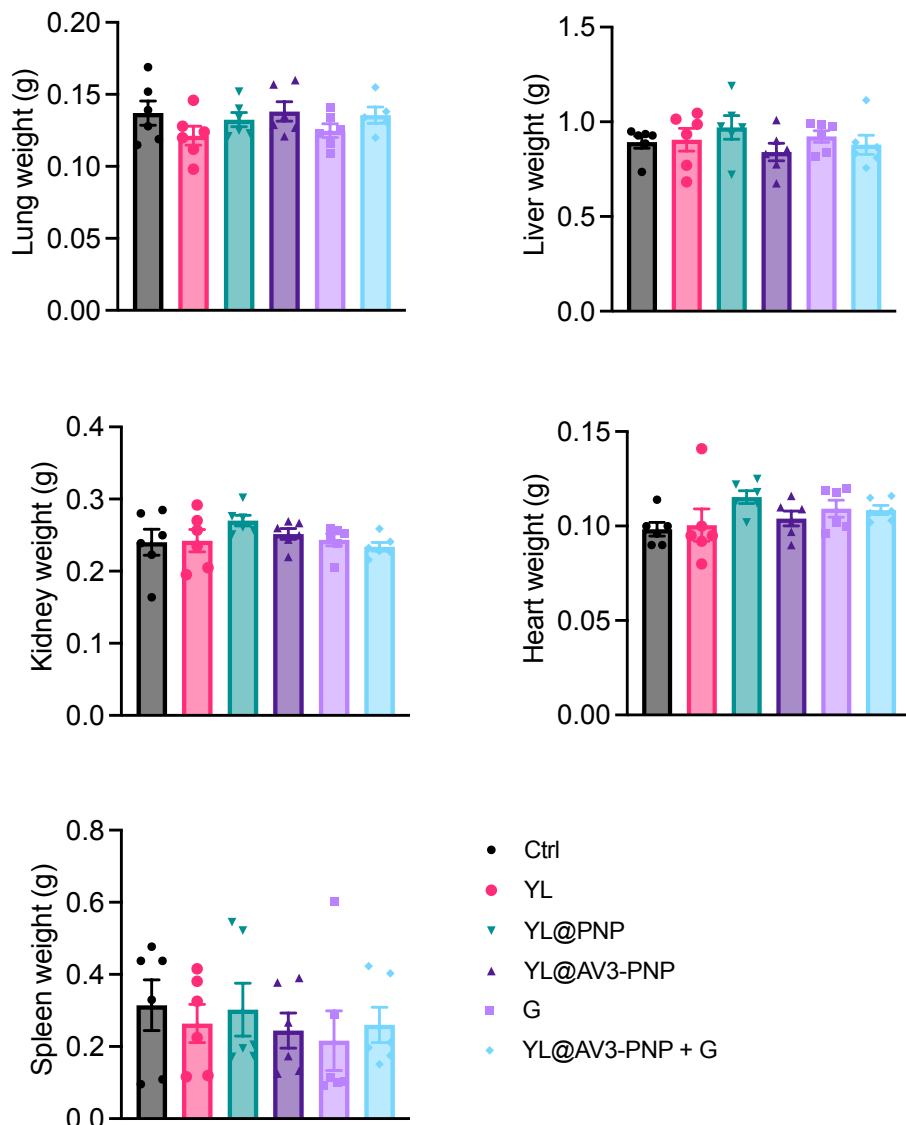
188

189

190 **Supplementary Figure 9.** Scatter graphs showing the effect of different treatments on the cellular phenotype
191 of CAFs including myCAF (FAP+ α -SMA+), iCAF (FAP+IL-6+ or FAP+CD26+).

192

193

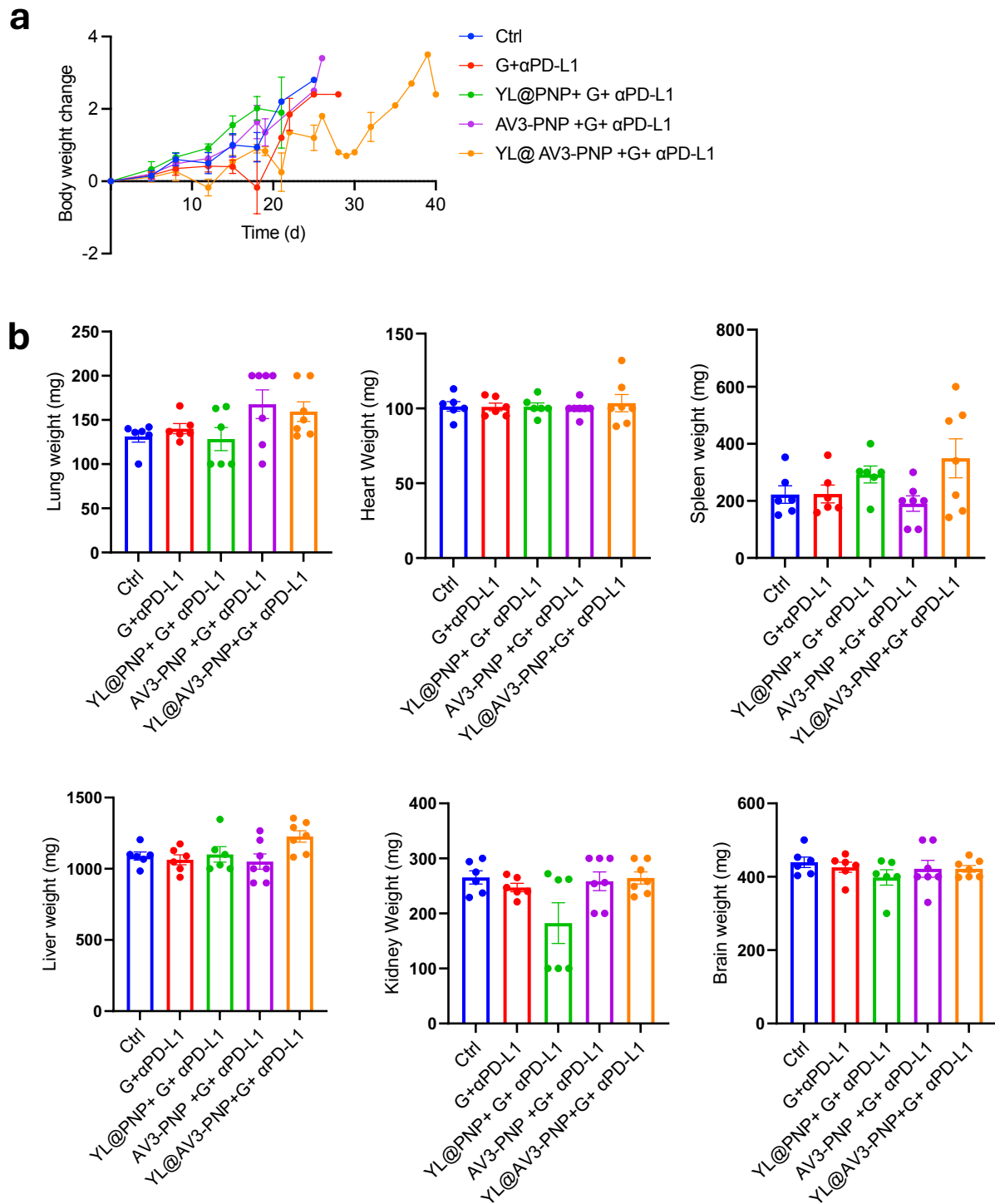


194

195 **Supplementary Figure 10.** Organ weight after different treatments in the KPC tumour model. Mice were
 196 treated with either PBS (Ctrl), YL-109 (YL; 5 mg/kg/d, i.p., t.i.w.), YL@PNP (equiv. 5 mg/kg/d, i.v., t.i.w.),
 197 YL@AV3-PNP (equiv. 5 mg/kg/d, i.v., t.i.w.), gemcitabine (G; i.p. 50 mg/kg/d, b.i.w.) or YL@AV3-PNP + G.
 198 Graphical data represent mean \pm s.e.m.

199

200



201

202 **Supplementary Figure 11.** Effect of different treatments on the body weight (a) and organ weights (b) in KPC
 203 mouse model. Mice were treated with either PBS (Ctrl), gemcitabine (G; 50 mg/kg/d, i.p., b.i.w.) and αPD-L1
 204 (200 µg/mouse/d, b.i.w.) and combination with YL@PNP, AV3-PNP or YL@AV3-PNP. YL in all formulations
 205 was 10 mg/kg/d, i.v., b.i.w. Graphical data represent mean ± s.e.m.